



Intelligent Hybrid Deep Learning Strategies for Optimizing Electric Vehicle Charging Infrastructure

Manjusha V.A¹, Sneha Narayanan², Sarika. S³

¹Lecturer, ²Lecturer, ³Head of the Department

¹Department of Electrical and Electronics Engineering, NSS Polytechnic college Pandalam, Kerala, India

²Department of Electrical and Electronics Engineering, NSS Polytechnic college Pandalam, Kerala, India

³Department of Electrical and Electronics Engineering, NSS Polytechnic college Pandalam, Kerala, India

Abstract: The integration of electric vehicles (EVs) into the modern transportation network necessitates advanced charging control and management systems to enhance efficiency and sustainability. In this study, we proposed a Hybrid Deep Learning (Hybrid DL) Mechanism for Charging Control and Management of EVs, which combines Recurrent Neural Networks (RNN) and Gated Recurrent Unit (GRU) techniques. In pursuit of robust feature extraction for battery information, we propose the utilization of RNNs. This approach aims to acquire comprehensive feature insights crucial for understanding the state of the EV battery. To further enhance predictive capabilities, we introduce a bidirectional GRU. The RNN-GRU hybrid model is designed to capture the temporal dependencies in EV charging patterns, offering improved prediction accuracy and real-time control capabilities. The benefits of this model include enhanced charging scheduling accuracy, faster response times to dynamic charging demands, and efficient energy utilization. The RNN component enables the model to learn from historical charging data, while the GRU component enhances the model's ability to adapt to changing EV usage patterns. By leveraging this hybrid approach, our model aims to make charging infrastructure more intelligent and adaptable, contributing to reduced energy costs, minimized grid impact, and a more sustainable EV ecosystem.

Index Terms - EVs, Hybrid Deep Learning, GRU, Battery State Prediction, Charging Infrastructure Optimization.

I. INTRODUCTION

EVs, vital for sustainability, align with the global shift towards renewable energy [1]. Balancing EV charging infrastructure optimization with power supply challenges is crucial [2]. This harmonizes human mobility with environmental balance, marking a decisive step towards a cleaner, greener future. EVs redefine the automotive landscape, with battery life intricately tied to factors like road conditions and driving styles [3]. Balancing energy consumption and operational demands is crucial for addressing challenges in battery storage [4]. Enhanced energy precision, extended lifespan [5], and improved recharging efficiency [6] are vital for sustainable and efficient electric transportation solutions. EREVs alleviate range anxiety by integrating an internal combustion engine as a generator, supplementing the battery [7]. HEVs optimize fuel efficiency with engine-generator series, enhancing flexibility and sustainability for adaptable and reliable transportation solutions. This marks a significant stride towards a greener and more energy-efficient future. The battery charger for EVs features a Power Supply Unit converting AC to DC [8], a Rectifier [9], and a Charging Controller [10, 11] ensuring optimal battery health by regulating voltage and current which is shown in fig. 1.

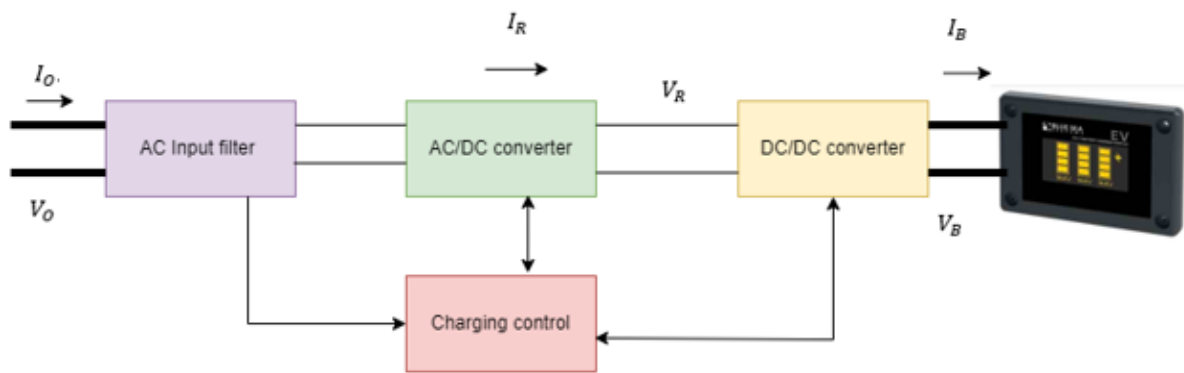


Figure 1: Block diagram of EV

The Battery Management System (BMS) is vital for EVs, monitoring SOC and temperature, optimizing battery performance, and ensuring safe charging [12]. It considers OCV [13], enhancing lifespan and efficiency. Effective charging infrastructure establishment, considering user behavior [14], is crucial for sustainable EV operation, addressing grid concerns and meeting market demands. A hybrid DL approach for EV state prediction employs RNNs and GRU, distinguishing between "outside" and "indoor" charging for tailored predictions. RNNs extract features, and GRU enhances predictive power, offering improved accuracy in forecasting diverse EV states, capturing long-term dependencies and dynamic charging behaviors.

II. LITERATURE REVIEW

Mazhar et al. [15] analyzed 3395 EV charging sessions, using machine learning (LSTM, DNN, KNN, RF, SVM, DT) for optimal control, reducing costs, and improving billing efficiency. Dataset limitations and ML advancements are noted. Ullah et al. [16] introduced pioneer ML algorithms for EV charging time prediction using ELM, FFNN, and SVR with GWO, PSO, and GA optimization. Notable features include SOC and A/C compressor. Kosuru et al. [17] presented IB-DRN, a DL system, achieving 98% accuracy in EV battery fault detection. Dataset enhances safety, suggesting future upgrades for models and monitoring. Hafeez et al. [18] suggested employing DL for data-driven demand-side management in a solar-powered EV charging station, enhancing reliability and reducing peak demand. Zafar et al. [19] presented HMDNN with MGO for accurate real-time SoC estimation in EVs, outperforming other methods with 0.1% NMSE and 0.3% RMSE, promising efficient monitoring. Haripriya et al. [20] employed ML and DL algorithms for EV lithium-ion battery aging prediction, favoring Naïve Bayes with 88% accuracy, enhancing driving range estimation. Jafari et al. [21] presented an extreme gradient boosting algorithm for accurate SOC estimation in EV lithium-ion batteries, handling nonlinear data effectively without initial SOC. Hong et al. [22] introduced a novel SOC prediction method for EV batteries using RDC and TA-LSTM, outperforming other algorithms. Potential for in-vehicle embedded systems is highlighted. Shi et al. [23] suggested a cloud-based AI framework using self-supervised transformer networks for co-estimating SOC and SOH in lithium-ion batteries, utilizing IoT devices for real-world data. Tian et al. [24] presented a DNN for precise SOC estimation in LiFePO₄ batteries, achieving <2.03% error. Integration with a Kalman filter enhances robustness and transfer learning adapts quickly. Dabbaghjamesh et al. [25] studied PHEV charging impact on MGs, using a decision-based algorithm addressing non-convexity. DLR constraints show variations in optimal dispatching.

III. MATERIALS AND METHODS

The proposed method employs a hybrid DL approach, utilizing RNNs for feature extraction and a bidirectional GRU for precise state prediction which is shown in fig 2. The simplified structure ensures efficiency, quick convergence, and outperformance of conventional SOC estimation models, validated through extensive real-world studies.

3.1 Dataset

The RNN-GRU approach uses the Kaggle ElectricCarDataClean.csv file from the mtcars dataset, featuring brand, charging, acceleration, powertrain, and plug type. Meticulous preprocessing ensures optimal user experience and accurate model training.

3.2 Preprocessing

Preprocessing is vital for model input preparation, addressing missing or duplicate data and irrelevant features. Techniques include encoding labels, removal of null values, and special character removal to ensure a clean dataset, enhancing machine learning model performance.

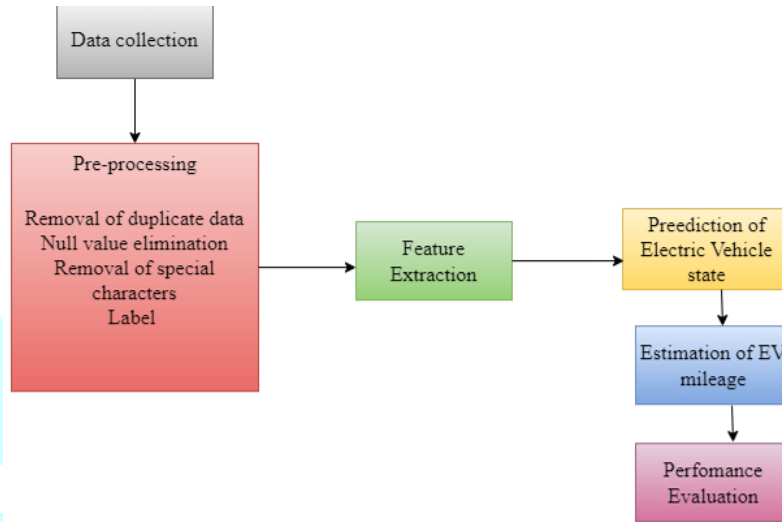


Figure 2: Proposed method for EV Operations

3.3 Feature Extraction with RNN

DL effectively tackles the intricate nonlinear behavior of EV batteries, preventing long-term prediction errors. Fig. 3 outlines the structure of a RNN. The RNN-based model produces state variables representing battery state information by capturing battery features.

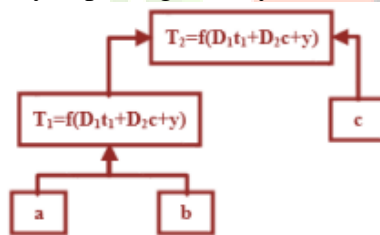


Figure 3: structure of an RNN parse tree

Moreover, for parent node computation, the research employed a neural network with weight matrices $D_1 \in O^{n \times n}$ and $D_2 \in O^{n \times n}$. Each parent node is considered to have a vector representation T_1 , and its calculation is determined by (1).

$$T_1 = f(D_1 a + D_2 b + y)$$

(1)

3.4 Forecasting the State of EVs through GRU

The GRU, a variant of RNNs, addresses long-term memory and gradient issues akin to LSTM. Fig. 4 shows GRU framework of the proposed method. In this study, GRU is chosen for its comparable performance to LSTM with lower computational costs. The GRU structure comprises the output, hidden state, reset gate, update gate, and current input. Subsequent process involves input, output, and hidden state components.

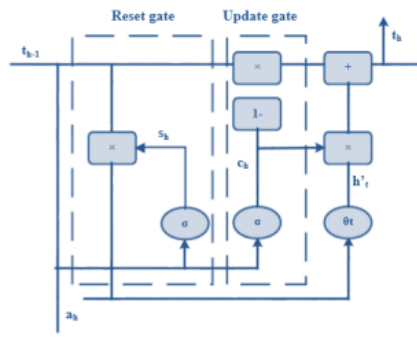


Figure 4: GRU Framework

3.4.1 Update gate

The update gate, denoted as c_h , regulates the incorporation of information from the prior moment into the current condition. A higher value of the update gate signifies an increased intake of information from the prior moment. The calculation for the update gate, c_h , is provided in equation (2).

$$c_h = \sigma(D_c, [c_{h-1}, a_h] + y_c)$$

(2)

The symbols y_c and D_c represent update gate bias and matrices weight. The sigmoidal function $\sigma(a) = 1/[1 + \exp(-a)]$ is employed in the equation, serving as a transformation that maps the input to values within 0 to 1, functioning as the gate controlling signal.

3.4.2 Reset Gate

The reset gate s_h governs the extent of information to be discarded from the previous hidden layer. Its computation is determined by employing equation (3).

$$s_h = \sigma(D_s, [c_{h-1}, a_h] + y_s)$$

(3)

In this, y_s and D_s represent reset gate bias and matrix weight, respectively. The reset gate's output is regulated by the sigmoid function, setting it to 0. Conversely, if the output is set to 1, all concealed states from the previous instance are preserved. Essentially, a lower reset gate value results in less information being retrieved from the previous state.

3.4.3 Output State

Compute the output state through a mathematical calculation t_h is in (4).

$$t'_h = \theta_t(D_t \cdot [s_h * t_{h-1}, a_h] + y_t)$$

(4)

Here, y_t and D_t refer to matrix weight and bias. The Hadamard Product function $*$, denoted by θ_t , scales the data to a range from -1 to 1 by multiplying corresponding matrix elements. The reset gate's output significantly impacts the resulting state of the GRU. The degree to which the neuron's output from the previous time step is preserved is contingent on the value of a_h , taking into account the current hidden layer state. Neuron's result is preserved to a greater degree when the a_h value is higher.

3.4.4 Hidden State

The t_h state of hidden layer, generated by the GRU, is determined by c_h , t_{h-1} and t'_h . Table I shows the description of terms used in the equation 5 and its mathematical representation provided as:

$$t_h = (1 - c_h) * t_{h-1} + c_h * t'_h$$

(5)

Table I: Description of terms in Equation (5)

Term	Description
t_h	Impact of $t_{(h-1)}$ on the output
t'_h	Influence of $t_{(h-1)}$ on the output
c_h	Higher c_h diminishes the impact of t_{h-1}
$(1 - c_h)t_{h-1}$	Selective "forgetting" of the prior hidden state
$t_{h-1}, c_h * t'_h$	Selective "memory" of the current node information
Forward GRU	Integrates information about moment h with the input sequence's earlier moment
Backward GRU	Incorporates information about moment h with the input sequence's later moment
Modified GRU	Incorporates data from both backward and forward directions of the input series
Two Hidden Layers	GRU units communicate information in opposing ways
Input a_h	Provides hidden layers working in multiple opposing ways at time h
Output y_h	Collaboratively determined by hidden layers at time h

The GRU's hidden layer propagation system is detailed in Equations (6)-(8). Table II shows the description of terms used in the following equations.

$$\vec{t}_h = f(\vec{D}a_h + \vec{P} \vec{t}_{h-1} + \vec{y}) \quad (6)$$

$$\overleftarrow{t}_h = f(\overleftarrow{D}a_h + \overleftarrow{P} \overleftarrow{t}_{h-1} + \overleftarrow{y}) \quad (7)$$

$$b_h = \alpha(\vec{t}_h, \overleftarrow{t}_h) \quad (8)$$

Table II: Description of terms in Equations from (6-8)

Term	Description
\vec{D}	Weight matrix representing connections between the hidden layer and the input layer in forward computations
\vec{P}	Weight matrix representing connections between the hidden layer and the input layer biases in forward computations
\overleftarrow{D}	Weight matrix representing connections between the hidden layer and the input layer in backward computations
\overleftarrow{P}	Weight matrix representing connections between the hidden layer and the input layer biases in backward computations
\vec{t}_h	Hidden-layer states in forward computations
\overleftarrow{t}_h	Hidden-layer states in backward computations
\vec{y}	Biases for forward calculations
\overleftarrow{y}	Biases for backward calculations
Hidden State	Incorporation of the hidden state in the model's capacity to interpret nonlinear data
Forward Dependencies	Capturing both forward and backward dependencies over time in the battery
GRU Structure	Logical approach for assessing the vehicle's condition
EV's State Prediction	Enabled by capturing both forward and backward dependencies over time in the battery

3.4.5 Estimation of the EV mileage

The GRU network is employed to compute the accumulated mileage, improving the estimation value in this study. The state and measurement functions for range estimation are expressed as equations (9) and (10). Table III shows the terms and its descriptions in equation 9 & 10.

$$R_{f,h} = R_{f,h-1} + \frac{EV_{h-1} + EV_h}{2} \Delta S + n_{h-1} \quad (9)$$

$$b_h = R_{m,h} + EV_h \quad (10)$$

Table III: Description of terms in Equation 9 & 10

Term	Description
ΔS	Sampling interval
$EV_{(h-1)}$, EV_h	EV speed measured at time steps $h-1$ and h
ob k	EV speed measured by the sensor
S	Output of the GRU network at time
$R_{f,h}$	Output range of the average speed technique at time h

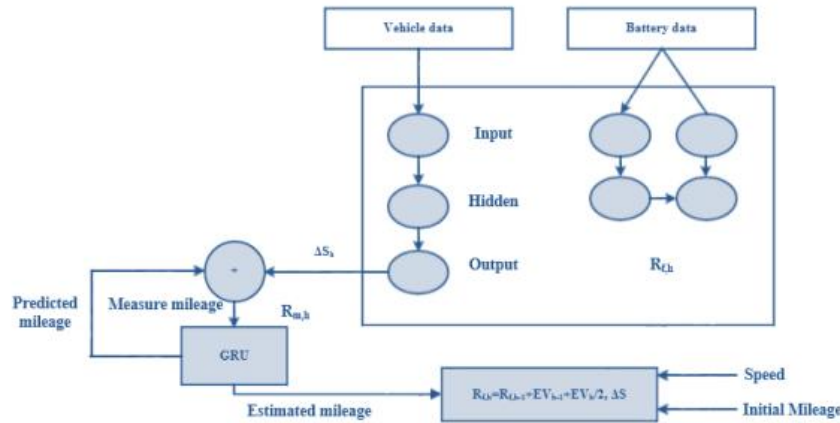


Figure 5: RNN-GRU methodology

3.5 Performance Metrics

In this study, the proposed method's predictive accuracy is assessed using regression metrics, including Mean Square Error (MSE) and Mean Absolute Error (MAE). Smaller values of MAE and MSE indicate better performance, signifying that the projected values closely align with the actual values. Equations (11) and (12) provide the definitions for MSE and MAE. Table IV shows the description of terms in the following equations.

$$\text{mean error square} = \frac{1}{M} \sum_{i=1}^M (b_i - \hat{b}_i)^2 \tag{11}$$

$$\text{mean absolute error} = \frac{1}{M} \sum_{i=1}^M |b_i - \hat{b}_i| \tag{12}$$

Table IV: Description of terms used in equation 11 & 12

Term	Description
b_i	Actual value
\hat{b}_i	Prediction value
M	Amount of sampling points

IV. RESULT AND DISCUSSIONS

The proposed method's efficiency is validated via rigorous testing along with simulations, with comprehensive battery feature extraction. The GRU-based prediction model accurately estimates and tracks EV mileage. Training with Adam optimizer showcases the RNN-GRU network's rapid convergence, emphasizing its ability to quickly capture the mapping relationship between input variables and mileage. Fig. 5 shows block diagram of RNN- GRU methodology of our study.

Table V: Comparison Of Various Methods

Methods	MSE	MAE
GRU	1.29	0.91
LSTM	0.80	0.72
ANN	9.80	2.30
MLR	4.01	1.77
RNN-GRU	0.92	0.70

Table V compares MAE and MSE, showing time series networks (RNN-GRU and LSTM) have lower values than traditional models (multivariate regression, tree-based, ANN). Fig. 6 illustrates RNN-GRU consistently outperforming other models, especially ANN, with minimal estimation error, validating its selection for superior accuracy in real-world scenarios.

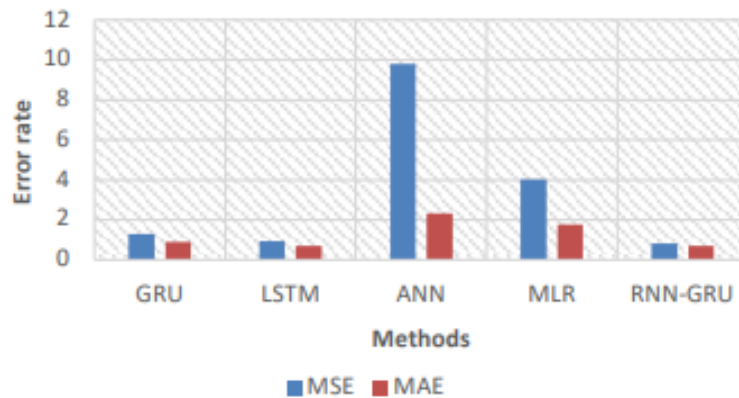


Figure. 6: Error Estimation of Different Models.

V. CONCLUSION

EV pose a challenge to conventional automobiles because of their eco-friendly nature and energy efficiency. Predicting states related to EV charging is crucial for anticipating consumers' charging needs, managing charging infrastructure effectively, and providing individualized charging capacity details determined by the locations of users. To address this, a hybrid DL approach is proposed for secure and dependable charging procedures, averting excessive charging or insufficient charging. The study employs RNNs to extract feature data on the battery and introduces a GRU for EV state prediction. GRU building on the RNN results, significantly enhances the model's efficiency with a simpler structure. Test results demonstrate the GRU technique's accuracy in tracking EV mileage. The hybrid DL algorithm exhibits fast convergence and reduced error rates compared to traditional models, showcasing its effectiveness through comprehensive real-world experiments.

REFERENCES

1. Yuan, Deling, Sun M, Zhao M, Tang S, Qi J, Zhang X, Wang K, Li B. Persulfate promoted ZnIn₂S₄ visible light photocatalytic dye decomposition. *Int. J. Electrochem. Sci.*, 2020; 15(2020): 8761-8770.
2. Wang K, Wang W, Wang L, Li L. An Improved SOC Control Strategy for Electric Vehicle Hybrid Energy Storage Systems. *Energies*, 2020;13(20):5297. <https://doi.org/10.3390/en13205297>.
3. Zhang Q, Li G. A predictive energy management system for hybrid energy storage systems in electric vehicles. *Electrical Engineering*, 2019;101(3):759–770. <https://doi.org/10.1007/s00202-019-00822-9>.
4. Ren G, Wang J, Chen C, Wang H. A variable-voltage ultracapacitor/battery hybrid power source for extended range electric vehicle. *Energy*, 2021; 231: 120837. <https://doi.org/10.1016/j.energy.2021.120837>.
5. Chu Y, Wu Y, Chen J, Zheng S, Wang Z. Design of energy and materials for ammonia-based extended-range electric vehicles. *Energy Procedia*, 2019;158:3064–3069.
6. Wen J, Zhao D, Zhang C. An overview of electricity powered vehicles: Lithium-ion battery energy storage density and energy conversion efficiency. *Renew. Energy*, 2020;162:1629–1648.
7. Chen N, Zhang P, Dai J, Gui W. Estimating the state-of-charge of lithium-ion battery using an H-infinity observer based on electrochemical impedance model. *Ieee Access*, 2020;8:26872–26884.
8. Al-Falahi, M. D., Tarasiuk, T., Jayasinghe, S. G., Jin, Z., Enshaei, H., & Guerrero, J. M. (2018). AC ship microgrids: Control and power management optimization. *Energies*, 11(6), 1458.
9. Li G, Xia J, Wang K, Deng Y, He X, Wang Y. A single-stage interleaved resonant bridgeless boost rectifier with high-frequency isolation. *IEEE J. Emerg. Sel. Top. Power Electron.*, 2019;8(2):1767–1781.
10. Luo L, Gu W, Wu Z, Zhou S. Joint planning of distributed generation and electric vehicle charging stations considering real-time charging navigation. *Appl. Energy*, 2019;242:1274–1284.

11. Zhang C, Greenblatt JB, MacDougall P, Saxena S, Prabhakar AJ. Quantifying the benefits of electric vehicles on the future electricity grid in the midwestern United States. *Appl. Energy*, 2020;270:115174.
12. Li, W., Rentemeister, M., Badeda, J., Jöst, D., Schulte, D., & Sauer, D. U. (2020). Digital twin for battery systems: Cloud battery management system with online state-of-charge and state-of-health estimation. *Journal of energy storage*, 30, 101557.
13. Essiet, I. O., & Sun, Y. (2021). Optimal open-circuit voltage (OCV) model for improved electric vehicle battery state-of-charge in V2G services. *Energy Reports*, 7, 4348-4359.
14. Hu, X., Liu, T., Qi, X., & Barth, M. (2019). Reinforcement learning for hybrid and plug-in hybrid electric vehicle energy management: Recent advances and prospects. *IEEE Industrial Electronics Magazine*, 13(3), 16-25.
15. Mazhar, T., Asif, R. N., Malik, M. A., Nadeem, M. A., Haq, I., Iqbal, M., ... & Ashraf, S. (2023). Electric Vehicle Charging System in the Smart Grid Using Different Machine Learning Methods. *Sustainability*, 15(3), 2603.
16. Ullah, I., Liu, K., Yamamoto, T., Shafiullah, M., & Jamal, A. (2023). Grey wolf optimizer-based machine learning algorithm to predict electric vehicle charging duration time. *Transportation Letters*, 15(8), 889-906.
17. Kosuru, V. S. R., & Kavasserri Venkitaraman, A. (2023). A Smart Battery Management System for Electric Vehicles Using Deep Learning-Based Sensor Fault Detection. *World Electric Vehicle Journal*, 14(4), 101.
18. Hafeez, A., Alammari, R., & Iqbal, A. (2023). Utilization of EV Charging Station in Demand Side Management Using Deep Learning Method. *IEEE Access*, 11, 8747-8760.
19. Zafar, M. H., Mansoor, M., Abou Houran, M., Khan, N. M., Khan, K., Moosavi, S. K. R., & Sanfilippo, F. (2023). Hybrid deep learning model for efficient state of charge estimation of Li-ion batteries in electric vehicles. *Energy*, 282, 128317.
20. Harippriya, S., Vigneswaran, E. E., & Jayanthi, S. (2022, August). Battery management system to estimate battery aging using deep learning and machine learning algorithms. In *Journal of Physics: Conference Series* (Vol. 2325, No. 1, p. 012004). IOP Publishing.
21. Jafari, S., Shahbazi, Z., Byun, Y. C., & Lee, S. J. (2022). Lithium-ion battery estimation in online framework using extreme gradient boosting machine learning approach. *Mathematics*, 10(6), 888.
22. Hong, S., Hwang, H., Kim, D., Cui, S., & Joe, I. (2021). Real driving cycle-based state of charge prediction for ev batteries using deep learning methods. *Applied Sciences*, 11(23), 11285.
23. Shi, D., Zhao, J., Wang, Z., Zhao, H., Eze, C., Wang, J., ... & Burke, A. F. (2023). Cloud-Based Deep Learning for Co-Estimation of Battery State of Charge and State of Health. *Energies*, 16(9), 3855.
24. Tian, J., Xiong, R., Shen, W., & Lu, J. (2021). State-of-charge estimation of LiFePO₄ batteries in electric vehicles: A deep-learning enabled approach. *Applied Energy*, 291, 116812.
25. Dabbaghjamesh, M., Kavousi-Fard, A., & Zhang, J. (2020). Stochastic modeling and integration of plug-in hybrid electric vehicles in reconfigurable microgrids with deep learning-based forecasting. *IEEE Transactions on Intelligent Transportation Systems*, 22(7), 4394-4403.